*Khalid Abdulhusain Mohammed**

Oil and Gas Department, College of Engineering, University of Thi-Qar, Thi-Qar, Iraq

Scientific paper
ISSN 0351-9465, E-ISSN 2466-2585
https://doi.org/10. 62638/ZasMat1528

Zastita Materijala 67 (2)
316 – 327 (2026)

The synergistic influence of chloride ion concentration and environmental temperature on the corrosion mechanisms of X65 carbon steel in CO_2-saturated oilfield environments

ABSTRACT

The longevity and safety of pipelines in the oil and gas sector rely on understanding how chloride ions influence corrosion in carbon steels exposed to CO_2-rich environments. This research investigates how different concentrations of chloride ions (1%, 3.5%, and 10% NaCl) affect the electrochemical response and corrosion behavior of X65 carbon steel under dynamic flow conditions. Corrosion rates were evaluated using weight-loss measurements, while surface characterization and phase identification were performed using scanning electron microscopy (SEM) and X-ray diffraction (XRD) analyses.Tests were conducted at temperatures of 30°C, 50°C, and 80°Cto closely simulate real-world oilfield conditions. The results show that chloride ions enhance ferrite dissolution, leading to the formation of an inner amorphous iron carbonate ($FeCO_3$) layer and an outer crystalline $FeCO_3$layer. While higher chloride concentrations increase the corrosive severity of the environment, they do not significantly alter the overall structure of the corrosion products. These findings provide new insights into CO_2 corrosion mechanisms in high-salinity environments and have practical implications for materials selection and pipeline maintenance in the oil and gas industry.

Keywords:*CO_2 corrosion,Corrosion kinetics, Pipeline integrity, Chloride ions, High-salinity environments, Localized corrosion, Produced water*

1. INTRODUCTION

Corrosion-induced pipeline failures pose a major challenge in the oil and gas industry, leading to safety hazards, structural weaknesses, operational inefficiencies, and significant economic losses. Carbon dioxide and chloride ions commonly found in produced water are major contributors to pipeline corrosion, especially in CO_2-rich environments. CO_2 dissolves in water, forming carbonic acid, which aggressively attacks carbon steel, while chloride ions exacerbate the corrosion by destabilizing protective oxide layers and promoting localized corrosion [1-7].

Despite extensive research on CO_2 corrosion, the role of chloride ions (Cl^-) at high concentrations (>3.5% NaCl) and their interaction with dynamic flow conditions in corrosion kinetics and product formation remains insufficiently understood.

While most existing research focuses on low-salinity conditions, acritical knowledge gap remains in understanding the mechanistic impact of chloride ions in high-salinity environments under flow conditions. This gap is particularly relevant because produced water from oil and gas wells often contains chloride concentrations exceeding 10%, creating highly aggressive environments for pipeline materials.

Produced water is a common byproduct of hydrocarbon production from both conventional and unconventional oil and gas wells. It is often reused in enhanced oil recovery through injection, making it essential in oilfield operations. However, due to its high chloride content, it can significantly affect materials and processes: the total dissolved solids (which include chloride) in produced water range from approximately 1 g/L to over 400 g/L, with many salinity levels reaching 10% (100 g/L) or more [8, 9].

Chloride ions in produced water accelerate the dissolution of the passivating surface film, initiate localized corrosion, and significantly alter the electrochemical behavior of corrosion products.

*Corresponding author: Khalid A. Mohammed
Email: dr.khalid@utq.edu.iq
Paper received: 12.07.2025.
Paper corrected: 28.07.2025.
Paper accepted: 29. 08.2025.

These effects compromise the structural integrity of the transportation systems, increasing the risk of failure and resulting in substantial costs for oil and gas operations [10].

Produced water contains various dissolved salts, with chloride (Cl^-), sulfate (SO_4^{-2}), and bicarbonate (HCO_3^-) as the primary anions, while sodium (Na^+), calcium (Ca^{2+}), and potassium (K^+) are dominant cations. Salts, in addition to corrosive gases such as carbon dioxide (CO_2) and hydrogen sulfide (H_2S), are commonly present in production streams. CO_2 in oil and gas wells originates from natural CO_2 gas and reservoir water. When dissolved in produced water, CO_2 forms highly corrosive species, including carbonic acid (H_2CO_3) and hydrogen ions (H^+), which severely degrade carbon steel structures[11].

Chloride ions can adsorb onto and penetrate the protective passive film on carbon steel, destabilizing the oxide layer and initiating localized corrosion such as pitting or crevice attack. Once the passive film is breached, pits or crevices can rapidly develop, leading to significant localized degradation. Additionally, chloride ions favor the formation of more soluble corrosion products compared to other halides, which can dissolve and expose fresh metal surfaces to ongoing corrosion. Consequently, carbon steel equipment, including pipelines, faces significant corrosion risks in the oil and gas industry[12, 13].

While extensive research has focused on uniform CO_2 corrosion, particularly under low-salinity conditions (≤3%) [14], studies in high-salinity environments remain limited. This highlights the critical need to further investigate the mechanisms of CO_2 corrosion at elevated salt concentrations.Liu et al. [1] demonstrated that CO_2 corrosion rates increase with rising chloride ion (Cl^-) content under constant temperature and CO_2 partial pressure. Their findings indicate that chloride ions accelerate anodic reactions and disrupt corrosion product films. However, they concluded that chloride concentration does not alter the chemical composition of corrosion products, although it affects their morphology and stability.

Elyian et al. [7] investigated the electrochemical behavior of API X100 steel in CO_2-saturated saline solutions with chloride concentrations ranging from 5 to 80 g/L. They observed peak corrosion rates at 15 g/L chloride, followed by a decline at higher concentrations, with a slight increase again at 20 g/L. Their findings suggest that chloride reduces the corrosion potential and significantly increases corrosion rates at 90°C. Additionally, the presence of oil inhibited corrosion by acting as a cathodic barrier.Qu et al. [15] studied the corrosion of magnesium alloy AZ31B in NaCl solutions saturated with CO_2. Their results showed that corrosion rates increased with NaCl concentration, as chloride enhanced the solution's conductivity and accelerated the dissolution of protective films on the metal surface.

This study addresses the knowledge gap by investigating the impact of chloride ion concentration on the corrosion behavior of X65 carbon steel (a material widely used in oil and gas pipelines) in CO_2-saturated environments. Corrosion tests were conducted at varying NaCl concentrations (1%, 3.5%, and 10%) and at temperatures of30°C and 50°C under dynamic flow conditions to simulate real-world pipeline environments. By integrating weight loss analysis, surface morphology characterization (SEM), and phase identification (XRD), this research provides new insights into how chloride ions influence the formation of corrosion products and overall material degradation. The findings not only enhance the scientific understanding of CO_2 corrosion but also inform practical strategies for mitigating pipeline corrosion in high-salinity environments.

2. METHODOLOGY AND EXPERIMENTAL PROCEDURE

X65 carbon steel, commonly used in the oil and gas sector, was used in this study. Its widespread application in transmission pipelines makes it a suitable choice due to its favorable mechanical and physical properties.

of X65 carbon steel

Table 1 presents the chemical composition of X65 carbon steel

Table 1.Chemical composition of X65 carbon steel (wt%) [16]

C	Si	Mn	P	S	Cr	Mo	Ni	Cu	Sn	Al	Nb	V	Fe
0.12	0.18	1.27	0.008	0.002	0.11	0.17	0.07	0.12	0.008	0.022	0.054	0.057	Bal

Corrosion Test Setup

The test setup was designed to replicate the dynamic flow conditions of transport pipelines, ensuring a realistic simulation of fluid flow. The layout and test section design are shown in Figure 1.Flow velocities were regulated by adjusting the pump's output rate. A Calpeda MX HL405/B horizontal multistage centrifugal pump was chosen

for the flow loop. Its wetted parts, constructed from corrosion-resistant materials, such as chrome-nickel-molybdenum stainless steel (AISI316L), prevented contamination of the aqueous solution during operation with brine, acidic, and highly ionized water at temperatures up to 80°C. Flow rates within the flow loop were controlled and measured using an Easymat5MT adjustable discharge valve and a SU7000 flow meter. The maximum allowable pressure of the pump is 8 bar. To maintain consistent temperatures during the testing period, a temperature controller unit monitored the aqueous solution. A CO_2 gas supply was connected to the flow loop tank to ensure continuous bubbling throughout the tests. In these experiments, the flow velocity was maintained at 5 m/s.

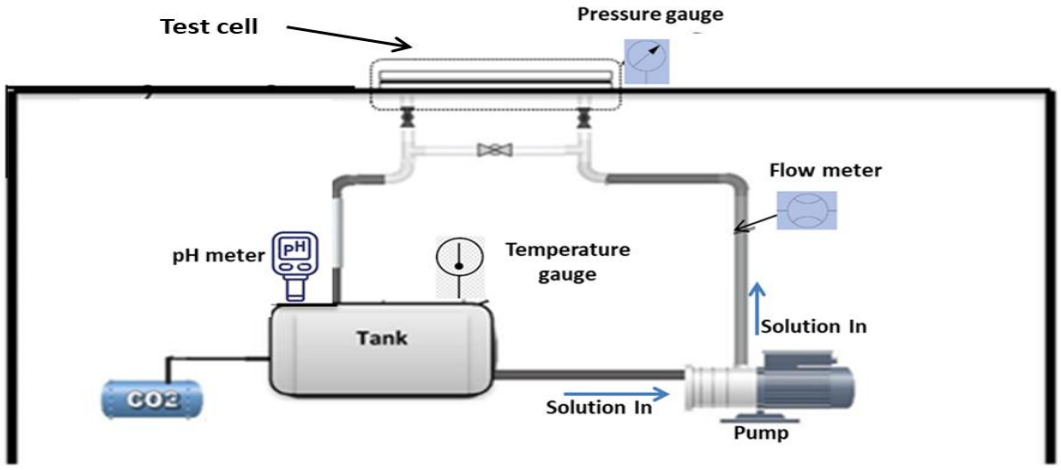

Figure 1.Schematic diagram of the flow loop and test section design.

Test Solution

Distilled water with varying NaCl concentrations served as the electrolyte. To reduce the oxygen levels below 10 ppm, CO_2 gas was used to purge the solution overnight prior to testing. Additionally, CO_2 gas was continuously bubbled through the solution during the experiments. Temperature and pH values were continuously monitored throughout the testing period, and sodium bicarbonate ($NaHCO_3$) was used to regulate the pH of the solution.

Test Material

X65 carbon steel samples were machined into cylindrical pieces (25 mm diameter, 10 mm thickness). The surfaces of weight-loss specimens were prepared prior to each experiment. They were wet-ground with silicon carbide SiC abrasive paper with a grit size up to 1200, degreased with acetone, cleaned with isopropanol alcohol, and dried using a hot air gun. A protective coating was meticulously applied to the top and outer edges of each sample. After curing, the prepared samples underwent another wet-grinding process and were weighed (m_1) using a precision digital balance accurate to 0.05 mg. The samples were then carefully placed in the flow cell and fitted into the sample holders.

Samples for corrosion rate measurements remained in the test cells for the full 168-hour experiment to ensure complete electrochemical data collection. For surface analysis, samples with coated surfaces were extracted from the test cell, stored in a vacuum environment until further examination.

Scanning electron microscopy (SEM) was used to analyze the effect of chloride concentration and temperature on the sample surfaces. Following that, the samples were weighed again (m_2) before removing the corrosion product layers using Clarke's solution (chemical composition is detailed in Table 2). A final weighing (m_3) was thenconducted to determine the mass of the samples after corrosion products had been removed.

Table 2. Chemical composition of Clarke's solution [16]

Component	Amount
Hydrochloric acid (HCl)	1000 ml
Antimony trioxide (Sb_2O_3)	20 grams
Stannous chloride ($SnCl_2$)	50 grams

3. RESULTS

Equation 1 was used to calculate the corrosion rate of the steel specimen throughout the experiment [16].

$$CR = \frac{87{,}600\,\Delta m}{\rho A T} \qquad (1)$$

where Δm is mass loss in grams, ρ is the density of carbon steel in g/cm^3, A is the exposed surface area in cm^2, and T is the test duration in hours. Each test was conducted in triplicate for consistency.

According to Figure 2, after the first 24-hour period, the corrosion rates remained nearly constant at 1.08 mm/y for experiments carried out in 1% and 10% NaCl at 30°C. In contrast, the test in 3.5 wt.%NaCl solution exhibited a significantly higher corrosion rate of about 1.55 mm/y. This inverse relationship between corrosion rate and salt concentration can be attributed to the inhibitive effect of salt, which suppresses both anodic and cathodic reactions, thereby slowing the overall corrosion process [17].

Throughout the 168-hour duration, corrosion rates in 3.5% and 10% NaCl solutions steadily increased, reaching approximately 1.70 mm/y. In contrast, for the 1% NaCl solution, the corrosion rate remained nearly stable at approximately 1.20 mm/y, with the temperature consistently maintained at 30°C. The slight decrease in corrosion rate is likely due to the accumulation of $FeCO_3$corrosion deposits.

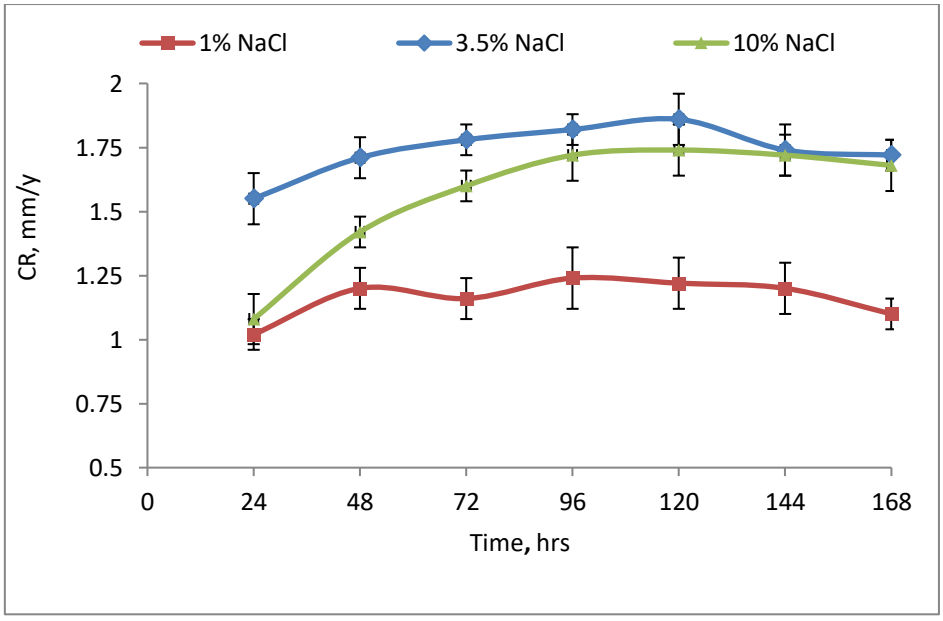

Figure 2.Corrosion rate of X65 carbon steel in 1%, 3.5%, and 10% NaClsolutions at 30°C.

Throughout the 168-hour test period, the bulk solution pH levels remained mostly stable across the three chloride ion concentrations investigated. Only slight variations in the pH of the bulk solution were observed, attributed to the changes in chloride ion levels, as shown in Figure 3. These findings align with previous studies [18, 19] that reported the influence of chloride ion concentration on solution pH.As observed by Guo et al.[20], the pH reading remains constant when the dissolution rate of metal (release of Fe^{2+}) equals the rate of iron carbonate formation at the surface. Enhanced iron dissolution leads to increased removal of hydrogen ions (H^+) from the surroundings, resulting in an electrical imbalance.

H^+ ions consumed during the cathodic reaction are supplied by H_2CO_3, which acts as a buffer. To restore charge neutrality, H^+ ions are removed at a certain rate but are also replenished depending on H_2CO_3activity, causing the pH to fluctuate accordingly.

Figure 4 (SEM images) and Figure 5 (XRD patterns) illustrate the effect of varying chloride concentrations on the formation and evolution of corrosion product layers in 1%, 3.5%, and 10% NaCl solutions at 30°C. The SEM images in Figure 4 and XRD patterns in Figure 5 confirm the formation ofiron carbide during the corrosion process under all three different chloride ion concentrations. This phenomenon is typically attributed to the selective dissolution of ferrite from the steel's surface layer, with no precipitation of corrosion deposits forming in the system [21-23]. SEM images after 168 hours reveal only slight variations in the overall corrosion morphology, indicating a consistent pattern of corrosion despite increasing concentrations of chloride ions.

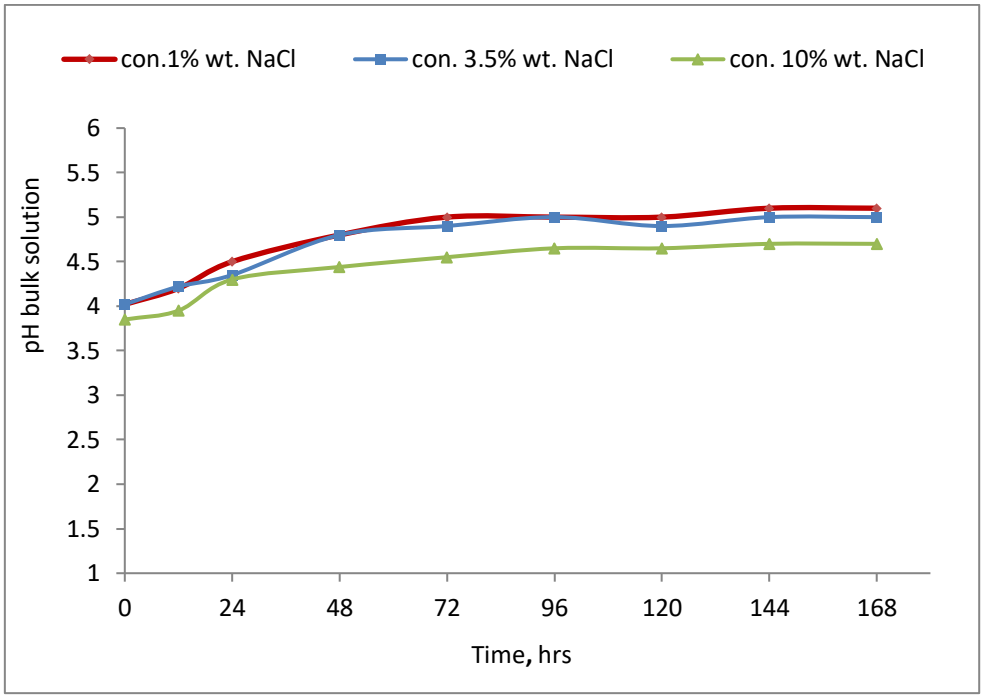

Figure 3. In-situ pH measurements of corrosion media with varying chloride ion concentrations at 30°C and a flow velocity of 5 m/s

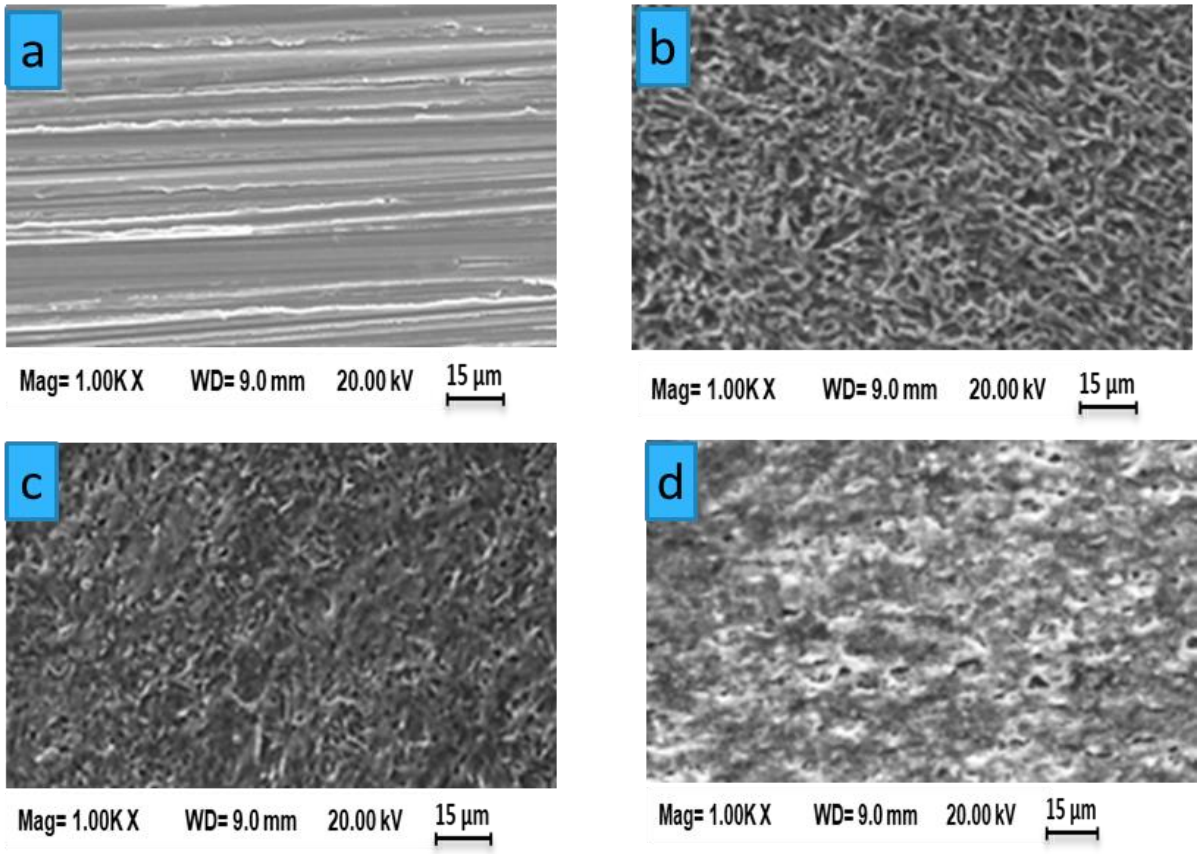

Figure 4. SEM images of corrosion products formed on the X65 carbon steel surface: (a) before testing, and after 168 hours of exposure at 30ºC in (b) 1%NaCl, (c) 3.5% NaCl, and (d) 10% NaCl solutions

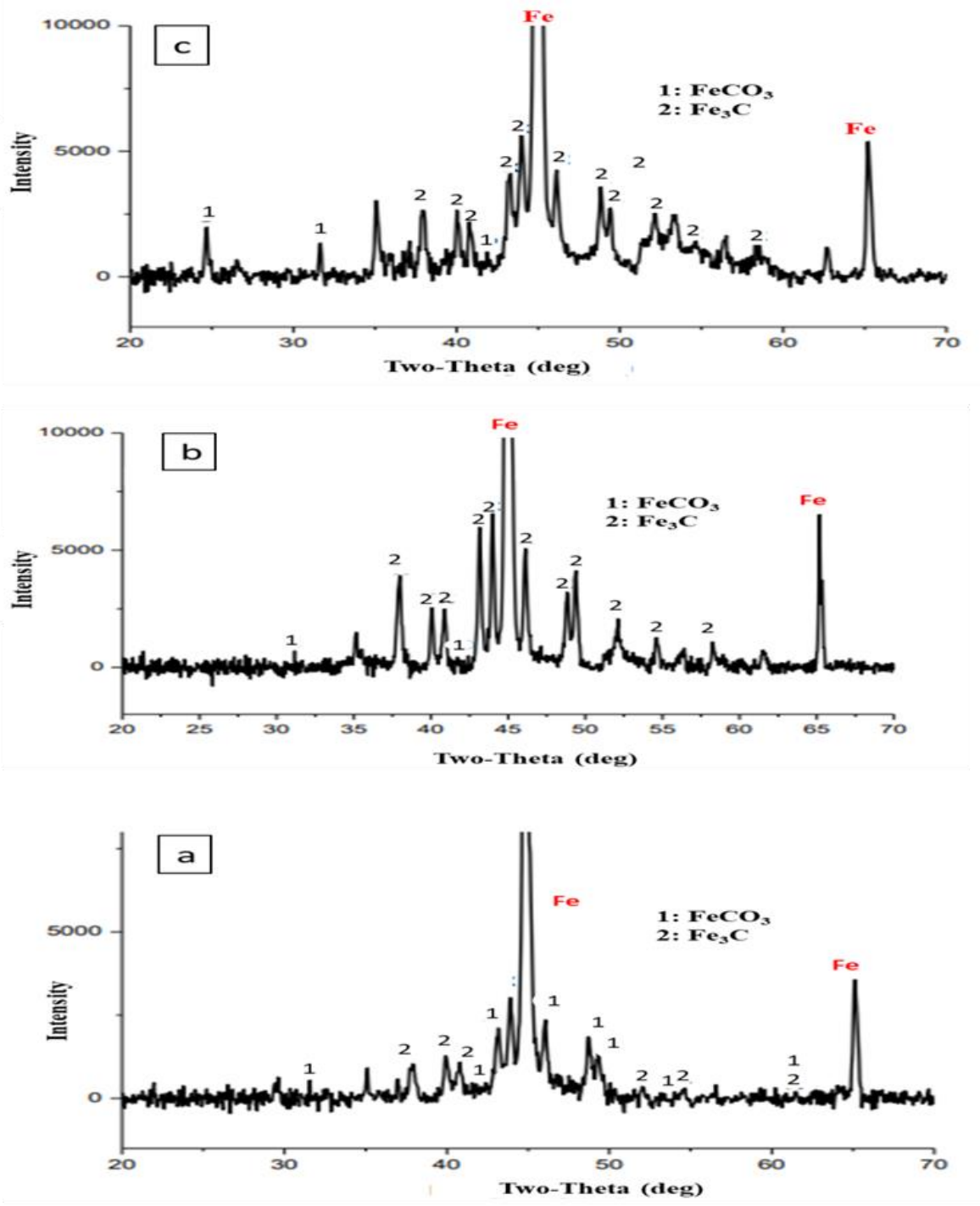

Figure 5. XRD patterns of corrosion products formed on X65 carbon steel after exposure at 30°C in (a) 1%, (b) 3.5%, and (c) 10% NaCl solutions.

Raising the test temperature to 50°C caused no significant alteration in the pH of the bulk solutions over the 168-hour test duration, as illustrated in Figure 6. These trends were consistent with those observed at 30°C. Additionally, the presence of 10% NaCl in the test solution resulted in a slightly lower solution pH, similar to the behavior observed at 30°C.

Sequential tests were conducted under flow conditions with NaCl concentrations of 1%**,** 3.5%**,** and10% at 50ºC, as shown in Figure 7**.** The resultsindicate that the initial corrosion rate in the 1%NaCl solution was about 1.75 mm/y, whereas corrosion increased to around 3.12 mm/year in the 3.5% and 10% NaCl tests.

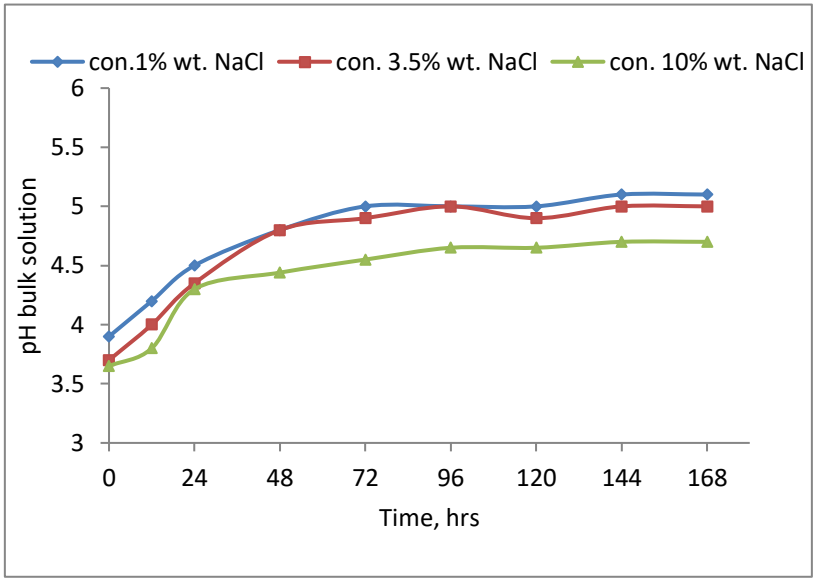

Figure 6. In-situ pH measurements of corrosive solutions at 50°C and a flow velocity of 5 m/s, under different chloride ion concentrations

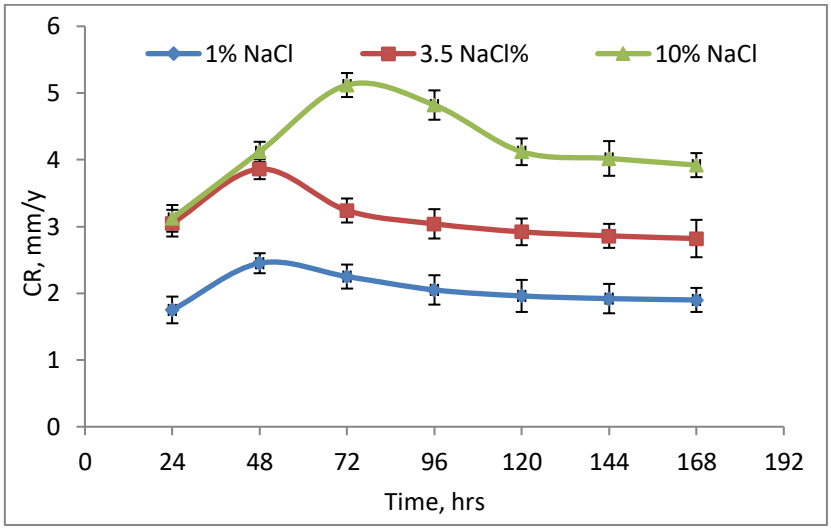

Figure 7. Corrosion performance of X65 carbon steel in 1%, 3.5%, and 10% NaCl solutions at 50°C

After 24 hours,corrosion rates increased for all tested salt concentrations, reaching their peak at approximately 48 hours.Beyond 48 hours, the corrosion rate declined in 1% and 3.5% NaCl solutions, decreasing from 2.45 mm/y to 2.25 mm/y and from 3.68 mm/y to 3.24 mm/y, respectively. However, in the 10% NaCl solution, the corrosion rate continued to rise, reaching 4.12 mm/y before peaking at 5.12 mm/y, followed by a gradual decline.

Between 72 and 168 hours, corrosion rates for all NaCl concentrations remained relatively stable. In the 1% NaCl solution, the rate gradually declined from approximately 2.4 mm/y at 72 hours to around 2.0 mm/y by the end of the test, suggesting the formation of a protective layer that slowed further corrosion. Similarly, in the 3.5% NaCl solution, the corrosion rate stabilized at around 3.2 mm/y from 72 hours onward, indicating that while some protective effects may have developed, the corrosion process continued at a moderate rate.

In contrast, the corrosion rate in the 10% NaCl solutionexhibiteda different pattern. It peaked at around 5.2 mm/y between 72 and 96 hours before declining. By the end of the test (168 hours), it had decreased to approximately 4.0 mm/y. This behavior suggests that high chloride concentrations initially accelerated corrosion but eventually contributed to the formation of a corrosion product layer, which gradually reduced the corrosion rate over time.

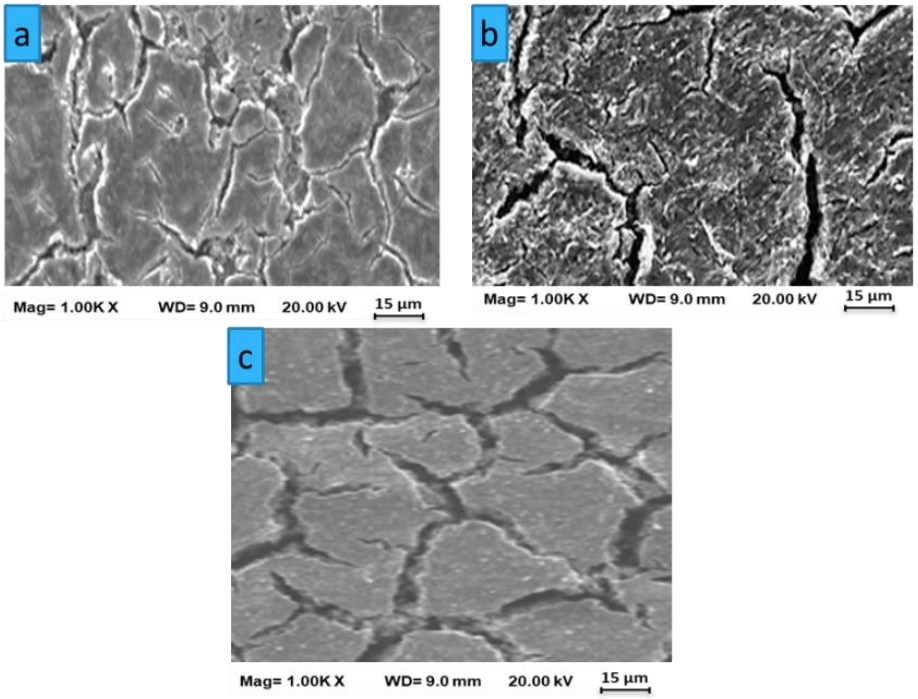

Figure 8.SEM images showing corrosion product layers on products on X65 carbon steel after 168 hours at 50°C in (a) 1%, (b) 3.5%, and (c) 10% NaCl solutions

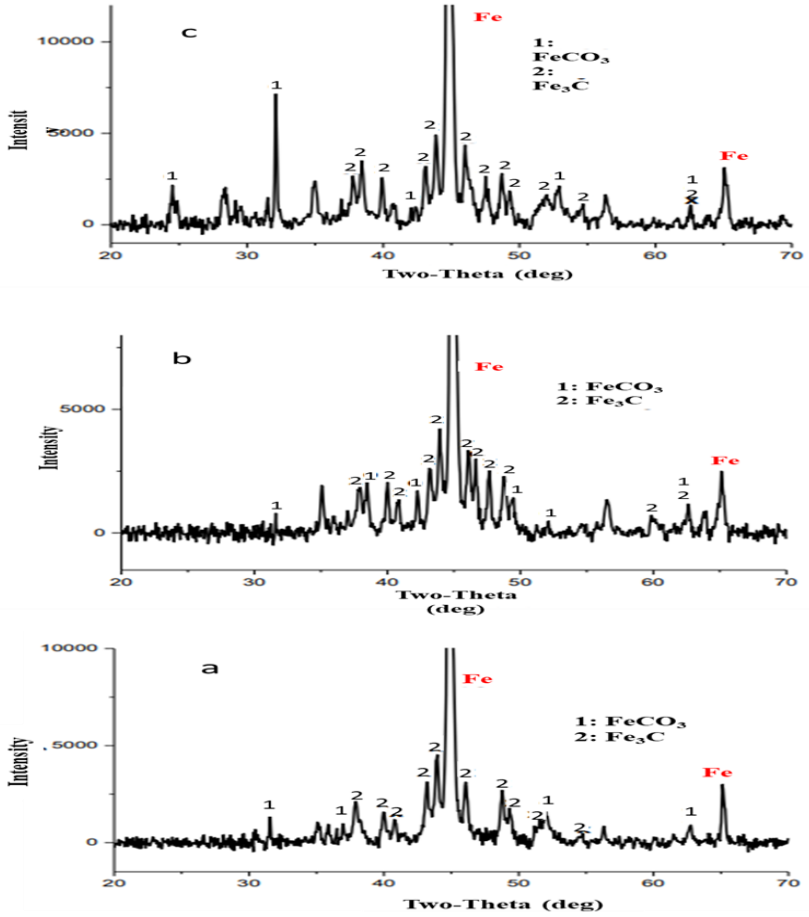

Figure 9. XRD Patterns of X65 carbon steel exposed to CO_2-saturated solutions for 168 hours at 50°C in (a) 1%, (b) 3.5%, and (c) 10% NaCl solutions

SEM images at 50ºC (Figure 8) suggest that chloride ions influence product layer development likethatobserved at 30°C. Iron carbide was the main surface phase detected across all tested chloride concentrations.The XRD pattern after 168 hours (Figure 9(a), (b), and (c)) confirmed the deposition of nano-structured polycrystalline iron carbonate on the steel surface in all chloride concentrations. Notably, the XRD pattern for the 10% chloride test reveals the presence of a nanoscale crystalline $FeCO_3$, whereas this evidence wasless pronounced in the SEM images for 1% and 3.5% chloride concentrations.

The corrosion performance of X65 carbon steel under flowing conditions was further investigated at 80ºC. Figure 10 illustrates how chloride levels influence the corrosion rate over time. At all three chloride ion concentrations, corrosion rates increased initially before reaching a plateau. From 96 hours until the end of the 168-hour test, the corrosion rate remained stable under flow conditions. Overall, the corrosion behavior throughout the test duration at 80ºC was similar to that at 50ºC. However, the stabilization period of the corrosion rate at 80ºC was shorter than that at 50ºC, particularly at 1% NaCl concentration.

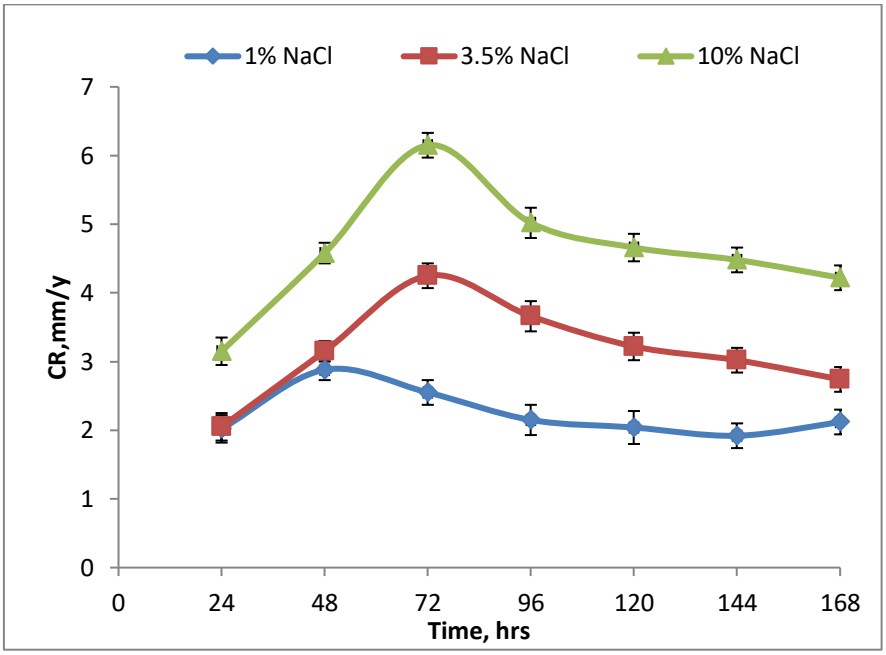

Figure 10. Corrosion rate of X65 carbon steel in 1%, 3.5%, and 10% NaCl solutions saturated with CO_2 at 80°C

Temperature Influence on the Corrosion Rate

At 30°C, the water dynamic viscosity (μ) is approximately 0.798 mPa·s, while at 80°C, it decreases to around 0.355 mPa·s. According to equation 2, the Reynolds number (Re) is inversely proportional to viscosity. As a result, the lower fluid viscosity at 80°C leads to a Reynolds number about 2.25 times that of 30°C, assuming the same flow velocity and channel geometry. Therefore, at 80°C, a higher mass transfer coefficient is expected, while achieving a similar amount of mass diffusion coefficient at 50°C is not possible.

Based on the Sleicher and Rouse correlation (equation 3), the mass transfer coefficient(K_m), is dependent on the Reynolds number and governs mass transfer between the bulk solution and the specimen surface. An increase in this coefficient enhances the diffusion rate of cathodic species to and away from the steel surface [24, 25].

$$Re = \frac{\rho v D}{\mu} \qquad (2)$$

where ρ is the density of water (kg/m³), v is the flow velocity (m/s), D is the characteristic length (m), and μ is the dynamic viscosity of water (Pa·s).

$$\frac{K_m * A}{D} = 5 + 0.015 * Re^a * Sc^b \qquad (3)$$

where K_m is the mass transfer coefficient, D is the diffusion coefficient, Sc is the Schmidt number, and A is the cross-sectional area of the sample.

High temperature accelerates the diffusion of species to and from the steel [26], leading to higher corrosion rates in high-temperature environments. This aligns with the present results, which indicate that corrosion rates at 80°C exceed those at 30ºC, as illustrated in Figure 11.

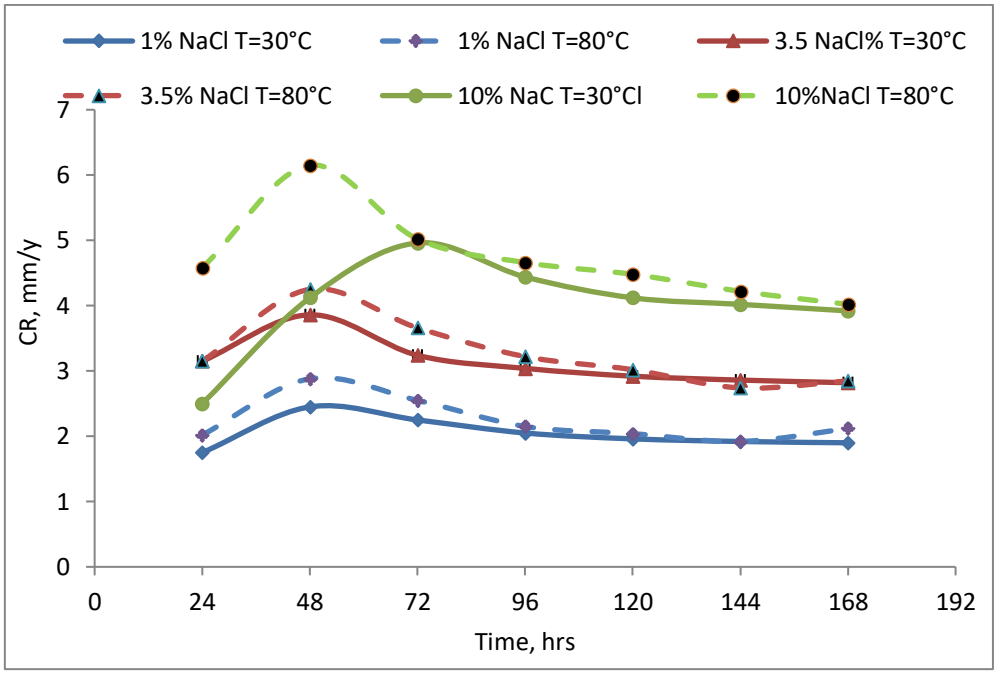

Figure 11.Comparison of the effect of temperature on corrosion rates at 30°C and 80°C in 1%, 3.5%, and 10% NaCl solutions

4. CONCLUSIONS

The synergistic effects of chloride ion concentration and temperature on the corrosion behavior of X65 carbon steel in CO_2-containing environments were investigated over 168 hours. The key findings are:

- Chloride Ion Effects: Higher chloride ion concentration accelerates the dissolution of ferrite in X65 carbon steel, promoting cementite formation. This results in the development of an inner amorphous $FeCO_3$ layer, followed by an outer crystalline$FeCO_3$ layer. However, chloride ion concentration did not significantly alter the overall $FeCO_3$ morphology.
- Temperature Effects: Raising the temperature from 30°C to 80°C increased the corrosion rate, particularly at higher chloride concentrations (10% NaCl). Corrosion rates then stabilized due to $FeCO_3$ formation, but the stabilization period was shorter at 80°C, especially at low chloride concentrations (1% NaCl).
- Corrosion Rate Trend: Corrosion rates initially accelerate, reach a peak, and then stabilize due to $FeCO_3$ deposition and the formation of nanoscale polycrystalline $FeCO_3$ layers. Higher chloride concentrations favored theformation of more crystalline $FeCO_3$. $FeCO_3$ also buffered the system by balancing H^+ ions consumption and replenishment.
- Mass Transfer and Material Selection: At 80°C, enhanced mass transfer accelerates rates of corrosion, emphasizing the need for careful material selection in high-salinity environments.
- Ferrite Dissolution: The presence of iron carbide across all chloride concentration regimes indicates selective ferrite dissolution.

Acknowledgments

The author is grateful to the Petroleum and Gas Department, Engineering College, and the University of Thi-Qar for their financial and scientific support.

5, REFERENCES

[1] Q. Liu, L. Mao, S. Zhou (2014) Effects of chloride content on CO2 corrosion of carbon steel in simulated oil and gas well environments, Corrosion Science, 84, 165-171.https://doi.org/10.1016/j.corsci.2014.03.025

[2] T. Yan, L.-C. Xu, Z.-X. Zeng, W.-G. Pan(2024) Mechanism and anti-corrosion measures of carbon dioxide corrosion in CCUS: A review, Iscience 27.https://doi.org/10.1016/j.isci.2023.108594

[3] K. Egab, K.A. Mohammed, A.K. Okab, S. Oudah(2020). Numerical Study of Condensation Heat Transfer and Droplet Dynamics on Different Wetting Surfaces of Gas Transportation Pipelines, IOP Conference Series: Materials Science and Engineering, IOP Publishing,p. 022105.DOI: 10.1088/1757-899X/928/2/022105

[4] A. Ndukwe, M. Deekae, W. Ejike, K. Okon, C. Ozoh, U. Chiemela, U. Ikele, I. Chibuzor, D. Ezeasia, I. Ikwuka(2025) Metal corrosion in high temperature conditions: A review, Zastita Materijala, 66, 292-312.DOI: https://doi.org/10.62638/ZasMat1203

[5] F. Xue, X. Wei, J. Dong, C. Wang, W. Ke(2019) Effect of chloride ion on corrosion behavior of low carbon steel in 0.1 M NaHCO3 solution with different dissolved oxygen concentrations, Journal of Materials Science &Technology, 35, 596-603. https://doi.org/10.1016/j.jmst.2018.10.001

[6] M. Li, A. Gross, B. Taylor, H. Zhang, J. Liu(2024), Effects of Cl-ion and temperature variations on steel corrosion in supercritical CO2 saturated aqueous environments, Process Safety and Environmental Protection, 187, 1446-1453. https://doi.org/10.1016/j.psep.2024.05.063

[7] F.F. Eliyan, F. Mohammadi, A. Alfantazi(2012)An electrochemical investigation on the effect of the chloride content on CO2 corrosion of API-X100 steel, Corrosion Science 64, 37-43. doi: 10.1016/j.corsci.2014.04.055

[8] K. Guerra, K. Dahm, S. Dundorf (2011).Oil and gas produced water management and beneficial use in the Western United States, US Department of the Interior, Bureau of Reclamation, Washington.

[9] C.J. Newell, J.A. Connor(2006). Strategies for addressing salt impacts of produced water releases to plants, soil, and groundwater, American Petroleum Institute Publication 4758.

[10] S. Nešić (2007) Key issues related to modelling of internal corrosion of oil and gas pipelines–A review, Corrosion science, 49, 4308-4338. https://doi.org/10.1016/j.corsci.2007.06.006

[11] S. Nešic, H. Li, J. Huang, D. Sormaz (2009) An open source mechanistic model for CO2/H2S corrosion of carbon steel, CORROSION 2009, OnePetro.https://doi.org/10.5006/C2009-09572

[12] Y. Peng, Y. Lin, R. Xia, Z. Dai, W. Zhang, W. Liu(2024). Electrochemical investigation of chloride ion-induced breakdown of passive film on P110 casing steel surface in simulated pore solution: behavior and critical value determination, Metals, 14, 93-102. https://doi.org/10.3390/met14010093

[13] H. Parangusan, J. Bhadra, N. Al-Thani(2021) A review of passivity breakdown on metal surfaces: influence of chloride-and sulfide-ion concentrations, temperature, and pH, Emergent Materials, 4, 1187-1203.https://doi.org/10.1007/s42247-021-00194-6

[14] H. Fang, B. Brown, S. Nešic (2010). High salt concentration effects on CO2 corrosion and H2S corrosion, NACE CORROSION, NACE,p. NACE-10276.https://doi.org/10.5006/C2010-10276

[15] Q. Qu, J. Ma, L. Wang, L. Li, W. Bai, Z. Ding(2011) Corrosion behaviour of AZ31B magnesium alloy in NaCl solutions saturated with CO2, Corrosion Science, 53, 1186-1193. https://doi.org/10.1016/j.corsci.2010.12.014Get rights and content

[16] K.A. Mohammed (2018) Experimental and theoretical investigation of top-of-the-line corrosion in CO2 gas and oil environments, University of Leeds.oai:etheses.whiterose.ac.uk:20479

[17] M. Singer, J. Al-Khamis, S. Nešić (2013) Experimental study of sour top-of-the-line corrosion using a novel experimental setup, Corrosion, 69, 624-638.https://doi.org/10.5006/0738E

[18] N. Anselmo, J. May, N. Mariano, P. Nascente, S. Kuri(2006) Corrosion behavior of supermartensitic stainless steel in aerated and CO2-saturated synthetic seawater, Materials Science and Engineering, A 428, 73-79. https://doi.org/10.1016/j.msea.2006.04.107

[19] C.-O. Olsson, D. Landolt(2003) Passive films on stainless steels—chemistry, structure and growth, Electrochimica Acta, 48, 1093-1104. https://doi.org/10.1016/S0013-4686(02)00841-1

[20] S. Guo, L. Xu, L. Zhang, W. Chang, M. Lu(2012) Corrosion of alloy steels containing 2% chromium in CO2 environments, Corrosion Science, 63, 246-258.https://doi.org/10.1016/j.corsci.2012.06.006

[21] M. Kermani, A. Morshed(2003)Carbon dioxide corrosion in oil and gas production compendium, Corrosion 59(8), 659–683. https://doi.org/10.5006/1.3277596

[22] J. Crolet, N. Thevenot, S. Nesic(1998) Role of conductive corrosion products in the protectiveness of corrosion layers, Corrosion, 54, 194-203. https://doi.org/10.5006/1.3284844

[23] J. Han, B. Brown, S. Nešic(2010) Investigation of the galvanic mechanism for localized carbon dioxide corrosion propagation using the artificial pit technique, Corrosion, 66, 095003-095003-095012. https://doi.org/10.5006/1.3490308

[24] C. Sleicher, M. Rouse(1975) A convenient correlation for heat transfer to constant and variable property fluids in turbulent pipe flow, International Journal of Heat and Mass Transfer, 18, 677-683.https://doi.org/10.1016/0017-9310(75)90279-3

[25] A.M. Nor, M. Suhor, M. Mohamed, M. Singer, S. Nesic2012 Corrosion of carbon steel in high CO2 containing environments-The effect of high flow rate, NACE CORROSION, NACE, pp. NACE-2012-1683.https://doi.org/10.5006/C2012-01683

[26] M.H. Nazari, S.R. Allahkaram, M. Kermani(2010) The effects of temperature and pH on the characteristics of corrosion product in CO2 corrosion of grade X70 steel, Materials & Design, 31, 3559-3563. https://doi.org/10.1016/j.matdes.2010.01.038

IZVOD

SINERGIJSKIUTICAJKONCENTRACIJEHLORIDNIHJONAI TEMPERATURE OKOLINENAMEHANIZMEKOROZIJEUGLJENIČNOG ČELIKAX65 U OKRUŽENJIMANAFTNIHPOLJAZASIĆENIM CO_2

Dugovečnost i bezbednost cevovoda u naftnom i gasnom sektoru zavise od razumevanja kako hloridni joni utiču na koroziju ugljeničnih čelika izloženih okruženjima bogatim CO_2. Ovo istraživanje istražuje kako različite koncentracije hloridnih jona (1%, 3,5% i 10% NaCl) utiču na elektrohemijski odgovor i ponašanje korozije X65 ugljeničnog čelika u uslovima dinamičkog protoka. Brzine korozije su procenjene merenjem gubitka težine, dok su karakterizacija površine i identifikacija faza izvršene pomoću analize skenirajućom elektronskom mikroskopijom (SEM) i rendgenskom difrakcijom (XRD). Testovi su sprovedeni na temperaturama od 30°C, 50°C i 80°C kako bi se što bolje simulirali uslovi na naftnim poljima iz stvarnog sveta. Rezultati pokazuju da hloridni joni pojačavaju rastvaranje ferita, što dovodi do formiranja unutrašnjeg sloja amorfnog gvožđe karbonata (FeCO3) i spoljašnjeg kristalnog sloja FeCO3. Iako veće koncentracije hlorida povećavaju korozivnost okruženja, one ne menjaju značajno ukupnu strukturu produkata korozije. Ova otkrića pružaju nove uvide u mehanizme korozije izazvane CO2 u sredinama sa visokim salinitetom i imaju praktične implikacije za izbor materijala i održavanje cevovoda u naftnoj i gasnoj industriji.

***Ključne reči**: CO_2 korozija, kinetika korozije, integritet cevovoda, joni hlorida, sredine sa visokim salinitetom, lokalizovana korozija, proizvedena voda*

Naučni rad
Rad primljen: 12.07.2025.
Rad korigovan 28.07.2025.
Rad prihvaćen: 29.08.2025

Khalid Abdulhusain Mohammed: https://orcid.org/0000-0002-0207-3479